Airflow Simulation of Particle Suction in Hard Disk Drives Manufacturing Process

Narongwit Yimsiriwatana and Thira Jearsiripongkul

Department of Mechanical Engineering, Faculty of Engineering, Thammasat University Rangsit, Pathumtani, Thailand 12121

Abstract

In Hard Disk Drive (HDD) particle is the major problem during the operation of HDD. Thus, in the HDD manufacturing process, particle is one of the important controlled parameters. In some processes the particle is removed from the HDD using suction tools. The designs of these tools affect the efficiency of particle removing process. Therefore, the prediction of the airflow induced by the suction tools becomes convenient and useful for the researchers to develop and improve each component of the tools and also the production. This project is to analyze the particle productivity and aim to improve it. In order to do so, the airflow simulation is needed to be done. The airflow is modeled and simulated using ANSYS CFX software. The results will lead the researchers and engineers to understand about the effect of each component and design of the suction tools to airflow and particle conductivity.

Keywords: Hard Disk Drive, Particle, and Suction tools

1. Introduction

The hard disk drive is one of the most important components in many computers these days and it is the primary device, which provides storage space for software and data. In today's hard disk drive industry, the demand for higher recording density and higher rotating speed has become more and more stringent. Thus, knowledge of flow dynamics is essential for designing a HDD that matches all the requirements above. Computational fluid dynamics (CFD) have been used by many researchers to simulate the aerodynamic design of disk drives.

First, M. Kazemi and A. Tokuda [1] studied the flow induced off-track vibration (FIV) of head-gimbal assembly (HGA) in HDD using CFD simulation software: Fluent, yielding the aerodynamic loads acting on different components of the head stack assembly (HAS). Those loads were then applied on a finite element model (FEM) of the HSA using ANSYS, and the transient response of the HSA was calculated.

Additionally, particles inside a HDD can cause performance degradation to the HDD via processes such as chemical erosion, scratch, etc, which may lead to inaccurate reading and writing of data or uncorrectable error. Thus, simulation of flow field and particle trajectories in HDD enclosures was conducted by H. Song, M. Damodaran and Quock Y. Ng [2]. The airflow

field and particle trajectories inside HDD are investigated in this study using commercial CFD software Fluent and Gambit. Three dimensional grids inside the HDD configuration are built using Gambit taking into account all the components and their geometric details. Based on the computed steady airflow patterns, particle trajectories are computed using routines available in Fluent as well as special particle trajectory functions defined by the user via the user-defined functions. Based on the investigation, the trajectory tends to be different according to sizes and materials.

D. Y. Lee, J. Hwang and G. N. Bae [3] also studied about the effect of contamination particles on the HDD. The slider disk interaction in contact-start-stop (CSS) mode is an important source of particle generation. They investigated the number and the sizes of particles generated in the hard disk drive, operating at increasing disk rotational speeds, in the CSS mode. CFD simulations were applied to obtain the free stream velocities for various spinning speed of the HDD. The increasing disk rotational speed directly affected the particle generation by slider disk interaction. The number of particles that were generated increased with the disk rotational speed.

Moreover, the Nano-scale Particle Tracking in HDD Cavity was studied by H. Kwon and H. J. Lee [4]. In this paper, the filter performance for particle collection is investigated with the effect of filter's permeability as well as the impact of air dam in HDD cavity. A simulation model is validated with the test results of cleanup time in two different cavity designs of HDD. A redesigned air dam is also found to be helping a recirculation filter collect more particles through tests and simulations.

In the HDD manufacturing process, particle is one of the important controlled parameters. Even though the manufacturing processes are done in the clean rooms, the particles may still exist. One main cause of the particles is the screw tightening process. These particles need to be removed from the HDD using suction tools. The designs of these tools affect the efficiency of particle removing process. Therefore, the prediction of the airflow induced by the suction tools becomes convenient and useful for the researchers to develop and improve each component of the tools and also the production. The main objective of this paper is to analyze the particle productivity and aim to improve it. In order to do so, the airflow simulation is conducted using ANSYS CFX software.

2. Theoretic

The set of equations which describe the processes of momentum, heat and mass transfer are known as the Navier-Stokes equations. These partial differential equations can be discretized and solved numerically. There are a number of different solution methods which are used in CFD codes. The most common, and the one on which CFX based, is known as the finite volume technique. In this technique, the region of interest is divided into small sub-regions, called control volumes. The equations are discretized and solved iteratively for each control volume. As a result, an approximation of the value of each variable at specific points throughout the domain can be obtained. In this

way, one derives a full picture of the behavior of the flow.

2.1 Governing Equations

2.1.1 The Continuity Equation

$$\frac{\partial \rho}{\partial t} + \nabla \cdot (\rho \boldsymbol{U}) = 0 \qquad \text{Eq. (1)}$$

Where ρ is the fluid density

U is the flow velocity

2.1.2 The Momentum Equation

$$\frac{\partial (\rho \boldsymbol{U})}{\partial t} + \nabla \cdot (\rho \boldsymbol{U} \otimes \boldsymbol{U}) = -\nabla p + \nabla \cdot \tau + \boldsymbol{S}_M \qquad \text{Eq. (2)}$$

Where the stress tensor, τ, is related to the strain rate by:

$$\tau = \mu \left(\nabla \boldsymbol{U} + (\nabla \boldsymbol{U})^T - \frac{2}{3} \delta \nabla \cdot \boldsymbol{U} \right) \qquad \text{Eq. (3)}$$

2.1.3 The Total Energy Equation

$$\frac{\partial (\rho h_{tot})}{\partial t} - \frac{\partial p}{\partial t} + \nabla \cdot (\rho \boldsymbol{U} h_{tot}) = \nabla \cdot (\lambda \nabla T) + \nabla \cdot (\boldsymbol{U} \cdot \tau) + \boldsymbol{U} \cdot \boldsymbol{S}_M + \boldsymbol{S}_E \qquad \text{Eq. (4)}$$

Where h_{tot} is the total enthalpy, related to the static enthalpy $h(T,p)$ by:

$$h_{tot} = h + \frac{1}{2} \boldsymbol{U}^2 \qquad \text{Eq. (5)}$$

λ Is the thermal conductivity

S_M is the momentum source

S_E is the energy source

The term $\nabla \cdot (\boldsymbol{U} \cdot \tau)$ represents the work due to viscous stresses and is called the viscous work term.

The term $\boldsymbol{U} \cdot \boldsymbol{S}_M$ represents the work due to external momentum sources and is currently neglected.

2.2 Particle Transport Theory

Particle transport modeling is a type of multiphase model, where particulates are tracked through the flow in a Lagrangian way, rather than being modeled as an extra Eulerian phase. The full particulate phase is modeled by just a sample of individual particles. The tracking is carried out by forming a set of ordinary differential equations in time for each particle, consisting of equations for position, velocity, temperature, and masses of species. These equations are then integrated using a simple integration method to calculate the behavior of the particles as they traverse the flow domain. The application of Lagrangian tracking in CFX involves the integration of particle paths through the discretized domain. Individual particles are tracked from their injection point until they escape the domain or some integration limit criterion is met. Each particle is injected, in turn, to obtain an average of all particle tracks and to generate source terms to the fluid mass, momentum and energy equations. Because each particle is tracked from its injection point to final destination, the tracking procedure is applicable to steady state flow analysis.

2.3 Forces Acting on the Particles

Several different forces affect the motion of a particle in a fluid. In CFX, the forces which have been included in the particle equation of motion are viscous drag, buoyancy force, virtual mass and pressure gradient forces, and the centripetal and Coriolis forces in rotating reference frames.

3. Simulation Conditions

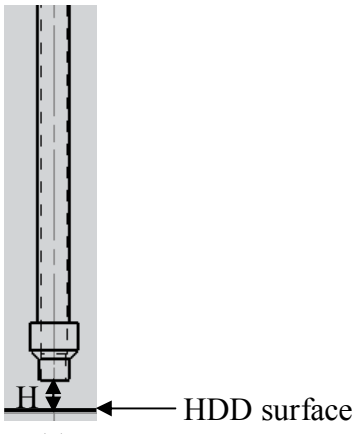

(a)

Fig. 1 Operating height of the suction tool model

The simulation was designed to test the particle removal efficiency of the suction tool at various operating heights (Fig. 1). The operating height (H) is the vertical distance between the suction tool tip and the target (the HDD containing particle). In this simulation, the test operating heights were 1 mm, 2 mm, 5 mm, and 10 mm.

The suction tool model was filled with the fluid domain required for the simulation. After that the suction tool model (solid part) was subtracted out. The remaining model was fluid only. The fluid model was then imported into ANSYS CFX software. The named selections were created at the inlet, outlet, and opening to be able to use the automatic tetrahedron inflation. The inflation is useful as it can capture the flow near walls and proximities. After that, the mesh was created using the automatic patch conforming technique with inflation. The advanced size function was enabled with proximity and curvature option turned on. As a result, the mesh resolution in proximity and curvature areas was finer. The resultant mesh elements are all tetrahedron as seen in Fig. 2(a) and the results of inflation and advanced size function applied can also be seen in Fig. 2(b).

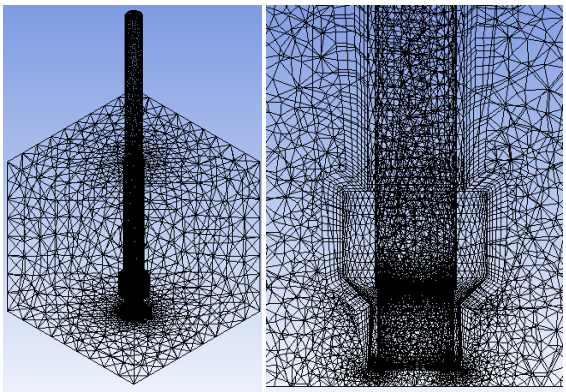

(a) (b)

Fig. 2 Mesh of the fluid used in CFX

According to the operating information from Seagate Company, the static pressure was initially set to -1.5 psi at the outlet where the vacuum pressure was applied. The particle would flow from the inlet, located on the HDD, to the outlet by passing through the suction tool. The areas where the fluid domain made contact with the suction tool were set to no-slip walls. The rests of the boundary were set to opening with the relative pressure of 0 Pa. The simulation reference pressure was set to 1 atm. The operating temperature was 25°C. The inlet mass flow rate was set to 1.74×10^{-6} kg/s as if the domain was initially almost motionless. For the forces acting on the particles, only pressure gradient, drag force, and buoyancy were presented. The pressure gradient resulted from the outlet boundary condition. The Schiller Naumann drag model was used to account for the drag force because it is suitable for sparsely distributed solid particles. The buoyancy effect was taken into account as a result of the density difference between the particle and the fluid.

Moreover, the fluid-particle coupling model was specified. To optimize CPU usage, two sets of identical particles were created. The first set consisted of 200 particles which were fully coupled. This allowed the particles to influence the flow field. The second set used one way coupling but contains 10000 particles. This provided a more accurate calculation of the particle volume fraction and local forces on wall, and higher resolution for the results. In both cases, particles were uniformly injected and equally distributed around the inlet boundary. The particles were aluminum whose density is 2702 kg/m^3. The initial mass flow rate of the

particles was set to be the same as one at the inlet boundary (1.74 x 10^{-6} kg/s). All particles were assumed to have the identical diameter of 0.15 micron. The particle erosion was not taken into account because it was not the observing parameter. The *k*-epsilon turbulence model was used because it offers a good compromise in terms of accuracy and robustness to the simulation. The thermal effect was neglected. The overall setting of the boundary conditions can be seen in Fig. 3.

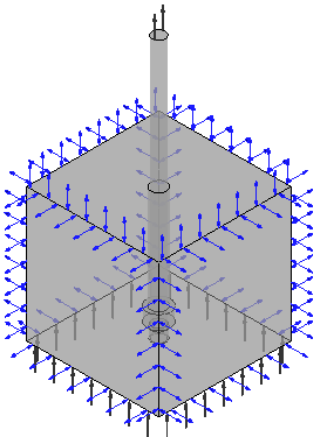

Fig. 3 Boundary conditions

After the Initial conditions and boundary conditions were all set, the CFX solver was run and the results were collected for the operating height of 1 mm, 2 mm, 5 mm, and 10 mm.

4. Results and Discussion

The results can be divided into two parts. The first part shows the effective area (in top view) in which the suction tool was able to remove the particles from the domain. The second part displays the velocity profile of the particles corresponding to each operating height. For both parts, they display only the particles which were taken out of the domain by the vacuum pressure at the outlet. Other particles that the suction tool was not capable of collecting are not shown so that the efficiency of the suction tool operated at various heights can be determined.

4.1 Effective Area

The corresponding effective area for each operating height is shown here in Fig. 4. Fig. 4(a) illustrates the initial locations of particles on the inlet boundary. Fig. 4(b), Fig. 4(c), Fig. 4(d), and Fig. 4(e) show the effective area of the suction tool operated at 1 mm, 2 mm, 5 mm, and 10 mm above the target respectively.

In Fig. 4(b), even though all the middle-area particles can be collected, the effective area is quite small due to very small operating height. Fig. 4(c) shows better and acceptable effective area. All the particles in the middle area can be collected as well as the particles around the area. For the 5 mm operating height, as seen in Fig. 4(d), the effective area is incredibly large and all particles in the middle area can also be collected. Thus, at this operating height, the suction tool had the excellent particle removal capability. Fig. 4(e) demonstrates the worst effective operating height of the suction tool. Some particles in the middle area were not removed but some particles in the distant area were collected instead.

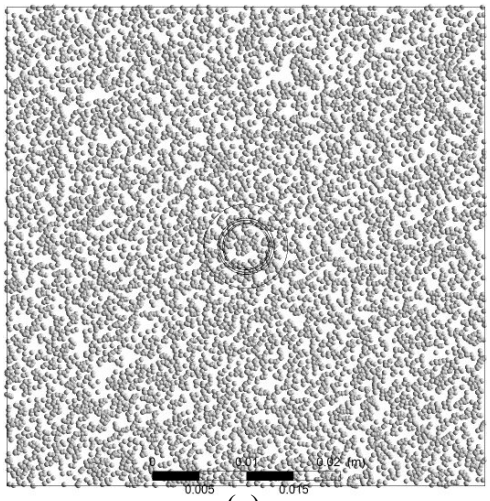

(a)

(b)

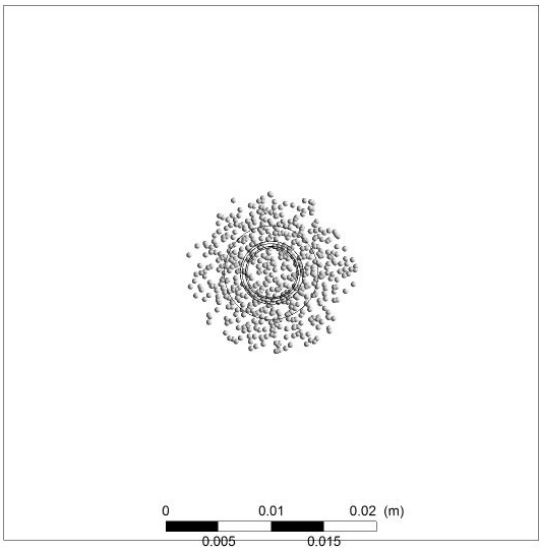

(c)

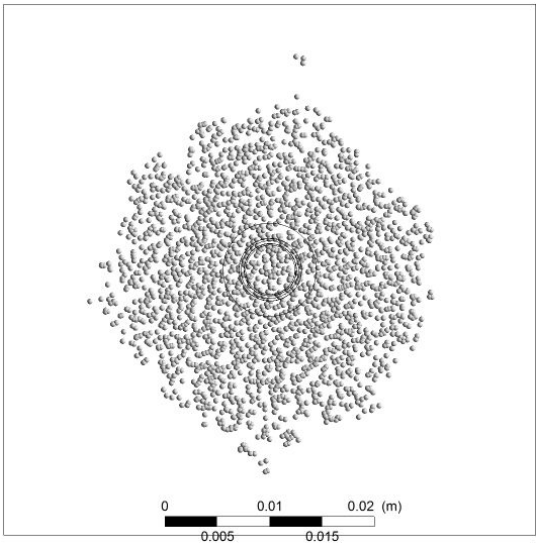

(d)

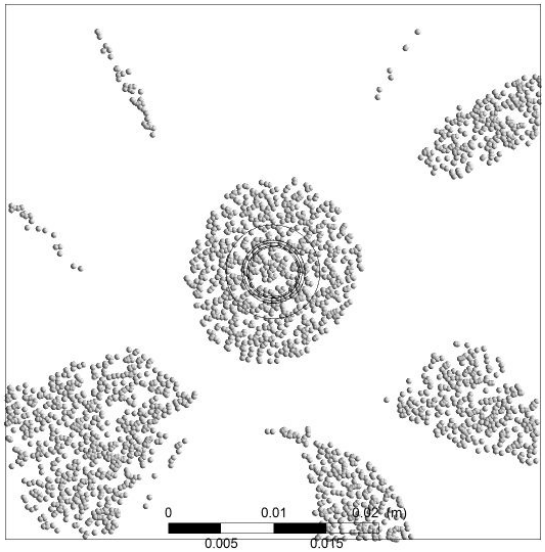

(e)

Fig. 4 Effective area

4.2 Particle Velocity Profile

The velocity profiles of the particles, describe how each particle traveled. For all profiles, the particles' velocity increased rapidly while they traveled from the initial point to the suction tool tip. The maximum velocity of the particle occurred just a little bit after it entered the suction tool tip. After that the velocity gradually decreased until the particle left the domain at the outlet. Fig. 5 shows the velocity profile inside the suction tool at the operating height of 1 mm. Because the velocity profile inside the suction tool for every operating height was not significantly different, only one is shown here.

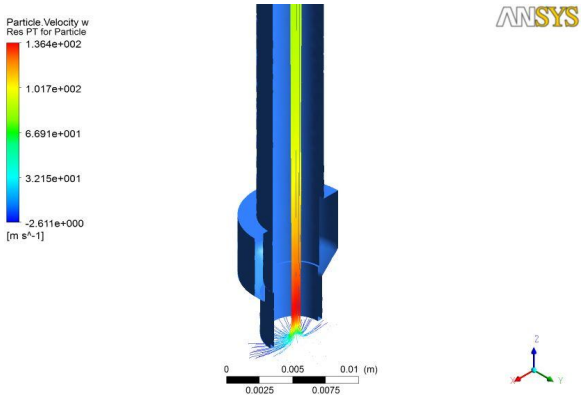

Fig. 5 The velocity profile inside the 1 mm operated suction tool

Although the velocity profile inside the suction tool is indifferent for all operating height, the profile outside the suction tool is not. Fig. 6 demonstrates how each operating height affected the velocity profile of the particle before entering the suction tool. Fig. 6(a), Fig. 6(b), Fig. 6(c), and Fig. 6(d) are corresponding for the operating height of 1 mm, 2 mm, 5 mm, and 10 mm above the target respectively.

It can be seen from Fig. 6(a) and Fig. 6(b) that the velocity profile of these two figures is almost identical except that the latter's profile is a little bit wider. Fig. 6(c) shows an incredibly larger profile. These three profiles are all steady. However, the profile for 10 mm operating height, shown in Fig. 6(d), is very much different. The swirling motion occurred as the distant particles were drawn into the suction tool while some of the particles in the middle area still left unhandled.

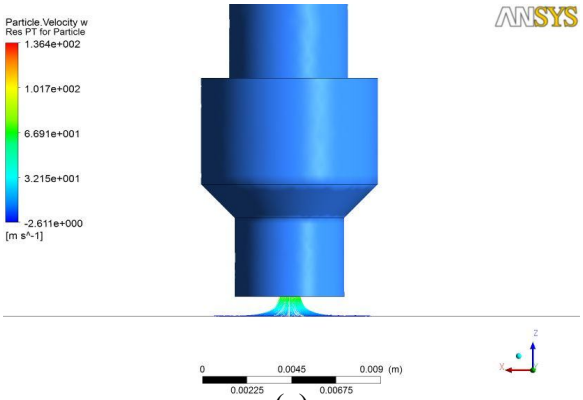

(a)

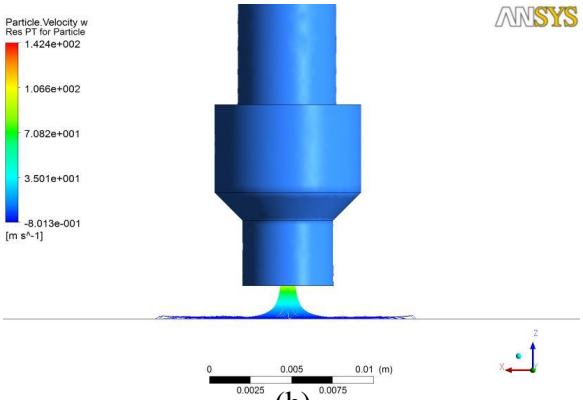

(b)

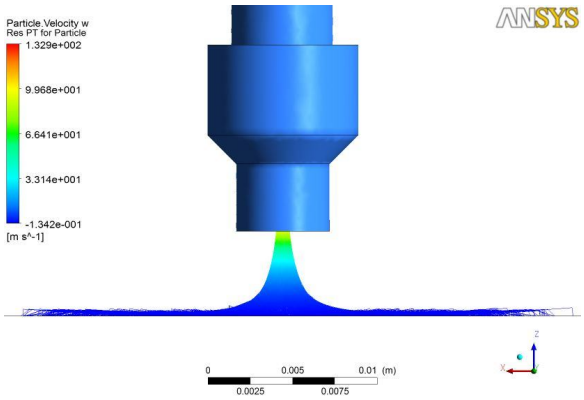

(c)

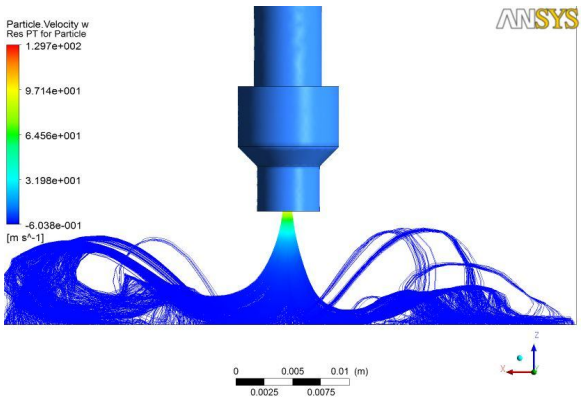

(d)

Fig. 6 The velocity profile before entering the suction tool

5. Conclusion

From the results, one can conclude that the most appropriate operating height for this suction tool design is at 5 mm above the target. For further improvement, the simulation results should be validated and compared with the experimental results in order to improve the accuracy of the simulation. After making sure that the simulation is robust, accurate, and reliable, this simulation technique will be able to be used as a tool for designing, developing, and improving each component of the suction tool. It can be done by testing the efficiency of each suction tool design at various operating conditions to find the optimum design. Ultimately, this would result in better particle

control and improvement of HDD manufacturing processes.

6. References

[1] M. Kazemi and A. Tokuda (2007), Investigation of Flow-induced Off-track Vibration of Head Gimbal Assemblies in Hard Disk Drives, paper presented in the *ASME Information Storage and Processing Systems Conference,* June 18-19, 2007, Santa Clara, CA, USA.

[2] H. Song, M. Damodaran and Quock Y. Ng, Simulation of Flow Field and Particle Trajectories in Hard Disk Drive Enclosures (2003), paper presented in the *1st Fluent CFD Conference for India and South East Asia*, Nov. 18-20, 2003, Pune, India.

[3] D. Y. Lee, J. Hwang and G. N. Bae (2004), Effect of Disk Rotational Speed on Contamination Particles Generated in a Hard Disk Drives, *Microsystem Technologies,* Vol. 10(2), January 2004, pp. 103-108.

[4] H. Kwon and H. J. Lee, Nano-scale Particle Tracking in HDD Cavity, HDD Lab, Samsung Information Systems America, USA

7. Acknowledgement

The authors would like to express gratitude for the generous support received from many individuals and companies whose contribution made this paper possible. Firstly, we would like to thank every professor and committee at the Faculty of Engineering, Thammasart University for useful knowledge, advice, and comments on this paper. In addition, we would like to thank our project cooperator, which is the Seagate Technology (Thailand), for technical support and information. Moreover, we appreciated the funding and support from FIBO/NECTEC (contract number: HAM - R & D 08 - 03 - 52 MF). Finally, we would like to thank to anyone who we did not mention above for any contribution to this paper.